

Estimation of In-situ Stress and Coal Bed Methane Potential of Coal Seams from Analysis of Well Logs, Ground Mapping and Laboratory Data in Central Part of Jharia Coalfield—An Overview

Prabir Kumar Pal, Suman Paul and Rima Chatterjee

Abstract Well log data of thirty (30) boreholes from central part of Jharia coalfield have been analysed for estimation of petrophysical and rock mechanical properties of coal seams to facilitate assessment of Coal Bed Methane (CBM) reservoir potentiality of those coal seam. Wells from Jharia area showed 18 major correlative seams, intersected between 214 and 1324 m depth. The resistivity, density and natural gamma ray log data from the wells of the study area have been utilized for:

- (a) Estimation of permeability of coal seams from resistivity log data;
- (b) Computation of in-situ stress magnitudes—vertical stress, effective vertical stress and effective horizontal stress at seam horizons;
- (c) Establish relationship between in-situ stress and permeability;
- (d) Estimation of gas content of coal seams and identification of most potential zones for CBM exploration.

It is observed that the permeability values ranging from 0.82 to 1.12 md with average gas content of 11.50 to 11.75 cc/gm. By comparing gas content, coal seam thickness as well as coal bed permeability of these major coal seams, the most viable CBM potential zone is mapped for this area.

Keywords CBM potential · Jharia coalfield · In-situ stress · Well log application

P.K. Pal
Integrated Coal Mining Limited, Kolkata, India

S. Paul
Department of Petroleum Engineering, Al Habeeb College of Engineering & Technology,
Hyderabad 501 503, India

R. Chatterjee (✉)
Department of Applied Geophysics, Indian School of Mines, Dhanbad 826004, India
e-mail: rima_c_99@yahoo.com

1 Introduction

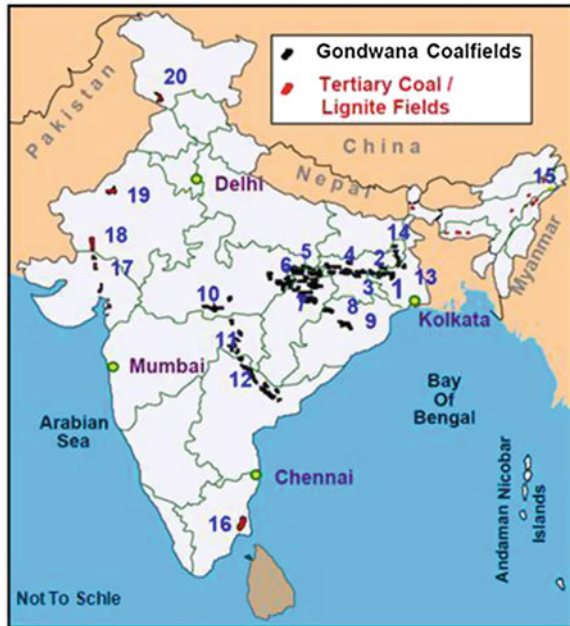
At present, methane is produced from coal beds in a number of sedimentary basins in Canada and USA, whereas in some other countries like China, Australia and India. Coal Bed Methane (CBM) is one of the exploration targets of the upstream petroleum sectors. Methane from coal represents a promising energy resource that has significant long-term prospective for discovery and development. On a global scale, the CBM potential of most major coal-bearing regions has been estimated to be 89–269 trillion m³ of gas in-place (Charles and Bai 1998). India having the fourth largest proven coal reserves and also being the third largest coal producer in the world, holds noteworthy prospects for profitable recovery of CBM. Coalfields of India are mainly divided into two groups namely; Gondwana (Permo-Carboniferous) and Tertiary coalfields. More than 98 % of the coal outputs of India are from Gondwana coalfields. These coalfields are distributed mainly in the river valleys of Damodar (West Bengal–Jharkhand), Pranhita Godavari (Maharashtra–Andhra Pradesh), Mahanadi (Orissa), Narmada (Madhya Pradesh) and Son (Madhya Pradesh). Geographical distribution of the major coal basins of India is shown in Fig. 1.

The performance of CBM reservoirs is extensively controlled by the density and aperture of natural fractures, particularly cleats in coalbeds and joints and in intervening shale and sandstone units (Pashin 1998; Pashin and Groshong 1998; Pitman et al. 2003). The development of joints and cleats in the coal bearing Formation is the product of regional tectonic stresses as well as internal stresses, generated by devolatilization of coal during thermal maturation (Close 1993; Law 1993; Laubach et al. 1998). It is, therefore, apparent that the geomechanical properties and permeability parameters need to be assessed for evaluating the economic potential of natural gas from coal seams of Jharia coalfield and the successful commercial production and exploration sites will be decided by those factors only.

Recent studies by different workers had indicated that India has an estimated resource base of virgin CBM (outside the mining areas) to the tune of 1.0–1.5 TCM (Hazra et al. 2003). The Jharia coalfield is the most important coalfield in India because in India this coalfield is now the sole repository of prime coking coals, i.e. coals which, with or without beneficiation, would on carbonization at high temperature, produce coke for metallurgical purposes. Hence, this coalfield has been extensively explored and exploited. This coalfield is still the leading contributor to India's coal production. Exploration for coal bed methane in Jharia Coalfield (JCF) has been going on for more than one decade.

Characterization and identification of coal seams in deep (more than 300 m) wells are generally considered as useful to evaluate CBM gas potential. The high methane reservoir potential of coal seams is due to the sub-optimum packing of its organic structure during coalification process. The density of pure carbon is approximately 2.23 gm/cc, whereas anthracite has around 1.35 gm/cc and bituminous coal 1.29 gm/cc (Li et al. 2003). This density contrast is almost completely

Fig. 1 Schematic diagram showing the locations of Gondwana coalfields and tertiary coal/lignitefields, India



| GONDWANA COALFIELDS | |
|--------------------------------|-----------------------|
| 1. Raniganj | 2. Jharia |
| 3. Bokaro | 4. North Karanpura |
| 5. Singrauli | 6. Sohagpur |
| 7. Korba | 8. Ib-valley |
| 9. Talchir | 10. Satpura |
| 11. Wardha | 12. Godavari |
| 13. Birbhum | 14. Rajmahal |
| TERTIARY COAL / LIGNITE FIELDS | |
| 15. Assam-Mehgalaya | 16. Neyveli |
| 17. Cambay | 18. Barmer-Sanchor |
| 19. Bikaner | 20. Jammu and Kashmir |

due to the micro-porosity created by the packing structure of the organic coal compounds. Harpalani and Schraufnagel (1990) reported that free methane, stored in the coal cleat network/fractures and joints, accounts for less than 10 % of the total gas enclosed in the coal and remaining 90 % plus of methane is physically adsorbed onto the surface of the pores of the coal.

It is claimed by the previous authors (Bell and Bachu 2003) that the worldwide resources of methane trapped within the porous coal system are greater than the total resources of all known conventional gas field. The commercial successes of CBM in the USA, Canada, Australia and China have also led to geophysical prospecting of the coal seams both in the mining and natural gas industry. In Indian scenario, the Gondwana coal seams of Damodar Valley are the prime targets for

CBM exploitation. Application of seismic survey for CBM prospecting to predict CBM content, estimation of mine pressure and other related aspects have been very limited in Indian mining industry. Therefore, the use of well logs in Jharia coalfield for estimation of the rock mechanical and petrophysical properties of coals and for in-situ stress analysis is a significant step to assess CBM potential of the coal seams and to identify high potential zones for CBM exploration and exploitation. Owing to the increasing importance of CBM production from gas reservoirs for coalbed methane extraction from target area like Jharia coalfield, the knowledge of coal bed permeability, in-situ stress magnitude, fracture orientation are essential for planning exploration and development because of their influence on recovery of methane, and the local and regional flow of methane gas and water within coal reservoirs.

To assess the potential of CBM reservoir, coal or non-coal core samples and well logs like density, gamma ray, and resistivity from wells have been used for quantitative estimation of petrophysical and rock mechanical parameters. In India, very few studies have been carried out to establish correlation of stress and permeability in CBM basins. In view of above, a fresh attempt has been made to develop a new methodology to decipher the in-situ stress direction acting at major coal seams from the available multiparametric well log data.

2 Study Area

The Jharia coalfield is situated in the eastern part of India, i.e. in Dhanbad district, Jharkhand and is located about 260 km northwest of Kolkata, West Bengal in the heart of Damodar Valley. The longer axis of this roughly sickle shaped coalfield is running northwest-southeast (Fig. 2). The Jharia coal basin located at the Singbhum craton extends for about 38 km in an east-west direction and a maximum of 18 km in north-south direction covering an area of about 456 km². Its regional strike is ENE to WSW in the western part which slowly swings to E-W in the middle and then to almost N-S towards eastern part of the coalfield. The dip of the Formation in general is southerly (10°). The general stratigraphic succession of Jharia coalfield is given in Table 1 (after Chandra 1992). Coal seams of Jharia coal basin occur in Barakar (Lower Permian) and Raniganj (Upper Permian) Formations within Lower Gondwana sequence (Chatterjee et al. 1990). The most important Barakar Formation (Lower Permian) of Jharia coalfield containing coal seams, consisting of fluvatile deposits as the lowermost member. The basement rocks mainly metamorphics are overlain by the Talchir Formation followed by the Barakar Formation which is the major coal-bearing horizon. The Barren Measures is overlying the Barakar formation followed by the coal bearing Raniganj Formation. The coal seams of the present study belong to Barakar Formation which does not show any evidence of high intensity tectonic deformation except normal gravity faults of different magnitudes—both minor (thrown less than 10 m) and major (thrown 10 m to greater than 100 m) (Ghosh and Mukhopadhyay 1985; Sengupta 1980). Out of total 30 major coal seams 18 are under Barakar Formation

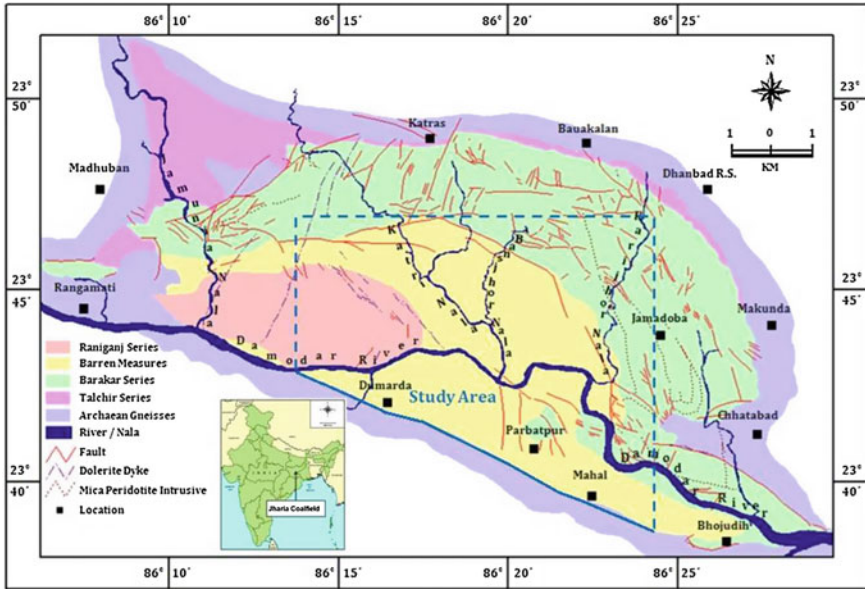


Fig. 2 Structural and stratigraphic map of Jharia coalfield, India (after Sengupta 1980) showing present study area

and the remaining 12 are under Raniganj Formation (Chandra 1992). It is important to note that Jharia coalfield is the only coalfield of India where source coal seams are of prime coking rank. The Barakar Formation consists of coal seams, conglomerates, shales, carbonaceous shales, coarse grained sandstones and siltstones. Data concerning organic petrology and thermal maturity of Barakar and Raniganj Formations are of considerable importance in determining the CBM potential in the Jharia coal basin. The vitrinite macerals are foremost in the shallower coals of Barakar Formation (Lower Permian) and range from 40 to 80 %, whereas exinite content vary in the range of 1–4 % and vitrinite reflectance value ranges from 0.83 to 1.69 % in Barakar coal seams of Jharia (Hazra et al. 2003). The volatile matters on dry ash free basis indicate that the Barakar coals of Jharia are high volatile bituminous to low volatile bituminous in rank (Rudra and Hazra 2009). It has been observed that generally ash content increases with consequent decrease in vitrinite content and increase in inertinite content for the Barakar coals of Jharia Coalfields. The inertinite content for deeper coals in Jharia is varying from 35 to 80 % and vitrinite content range from 20 to 62 % (Hazra et al. 2003).

The present study area, consisting of Singra, Kapuria, Barki, Dumarda, Parbatpur and Moonidih (Extension)/Jarma blocks covering an area of about 38 km² is located in the south-central part of Jharia coalfield (Fig. 2). Available well logs, litho-logs and core samples of total 30 exploratory wells have been considered for present study. Figure 3 displays locations of 30 exploratory wells in the study area.

Table 1 Generalized stratigraphic sequence of Jharia coalfield, India

| Age | Group | Formation | Litho-type | Max. thickness (m) |
|-----------------------|----------------------------|---|--|--------------------|
| Recent and sub-recent | | Weathered | Alluvium, sandy soil, clay, gravel etc. | 30 |
| <i>Unconformity</i> | | | | |
| Jurassic | | Deccan trap and other igneous activity (intrusives) | Dolerite dykes, mica lamprophyre dyke and sills | |
| <i>Unconformity</i> | | | | |
| Upper Permian | D A M U D A | Raniganj | Fine grained feldspathic sandstones, shales with coal seam | 800 |
| Middle Permian | | Barren measure | Buff colored sandstone, shales and carbonaceous shales | 730 |
| Lower Permian | | Barakar | Buff colored coarse to medium grained feldspathic sandstones, grits, shales, carbonaceous shales and coal seam | +1250 |
| Upper Carboniferous | | Talchir | Greenish shale and fine grained sandstones | 245 |
| <i>Unconformity</i> | | | | |
| Archaeon | | | Metamorphics | |

After Chandra (1992)

The 30 wells, namely, S1, S2, S4, S5, S7, S8, S10, S13, S14, K1, K4, K5, K8, K10, K11, K12, K14, K16, K17, K19, J1, J2, J3, J4, J6, J7, J8, M1, M2 and M3 (Fig. 3) have been considered for estimation of stress magnitude and permeability from well log data. Physical properties of coal like permeability and porosity have generally been determined from limited sample volumes such as plugs or cores. There is no published data available on the physical properties of the coal seams in and around the study area. Therefore a methodology has been proposed for estimation of permeability of the coal seams with macro-cleat system from the well log-derived porosity and from known cleat spacing of the coal seams around the study area. Well log data, coal core samples and geological litho-logs of these boreholes recorded occurrence of 18 major/consistent coal seams, namely, seam A, B, C, D, E, F, G, H, I, J, K, L, M, N, O, P, Q and R of Barakar Formation at different depths varying between 214.58 m (in seam R for well K4) and 1354.24 m (in seam J for well J4) in the study area.

It is necessary to correlate the major seams encountered in the wells to evaluate seamwise properties from 30 wells, distributed over the study area (Fig. 3). A schematic regional cross-section along the section K8-S8 (Chatterjee and Paul 2013) traversing the seven wells; K8, K10, K1, J3, J4, S5 and S8 (Fig. 4) show the correlation of the major seams considering both geophysical logs and geological

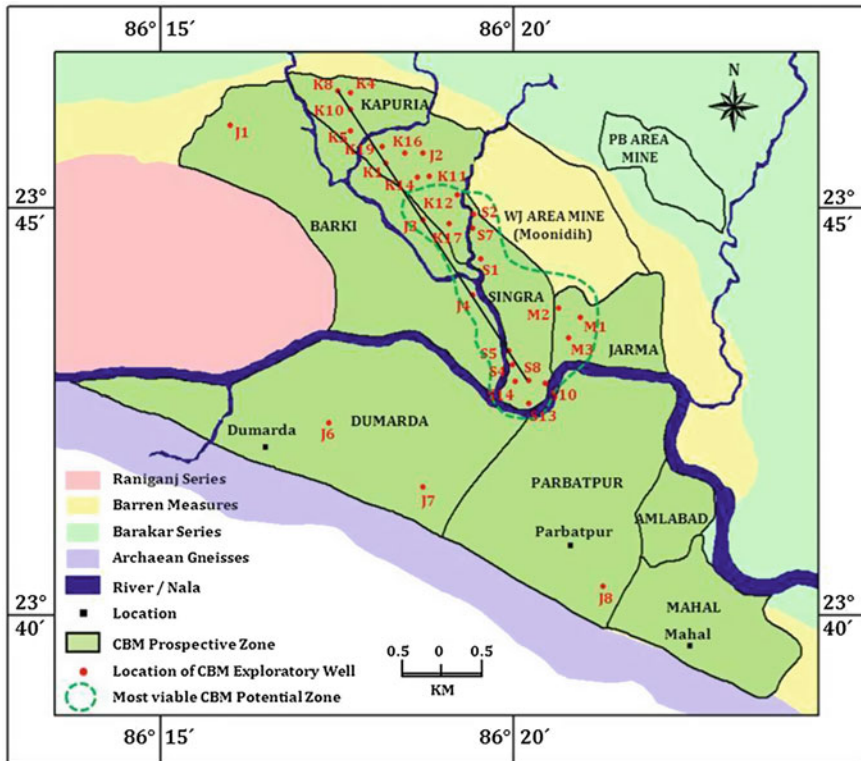


Fig. 3 Showing locations of 30 numbers of wells are distributed in Singra, Kapuria, Jarma, Parbatpur, Dumarda and Barki areas and also locations of WJ area and PB area underground coal mines of Jharia coalfield

litholog data. This cross section across the study area reveals the structural lay out of the seams in the study area. The structure of whole Jharia coal basin had been reported by previous workers like Sengupta (1980) and Chandra (1992).

3 Proximate Analysis of Coal in Laboratory

About 141 coal core samples were collected from the 10 wells, such as: wells S4, S5, S9, S15, S21 from Singra block and wells K9, K10, K16, K19 and K24 from Kapuria block of the Jharia coalfield (Fig. 3). Coal samples were collected following the Indian Standard procedure (IS 436 (Part 1/Section 1) 1991). Proximate analysis based on the Indian Standard procedures (IS 1350 (Part 1) 2003) was carried out in the Fuel and Mineral Engineering (FME) Laboratory of Indian School of Mines, Dhanbad. Table 2 provides the seam-wise proximate analysis results from

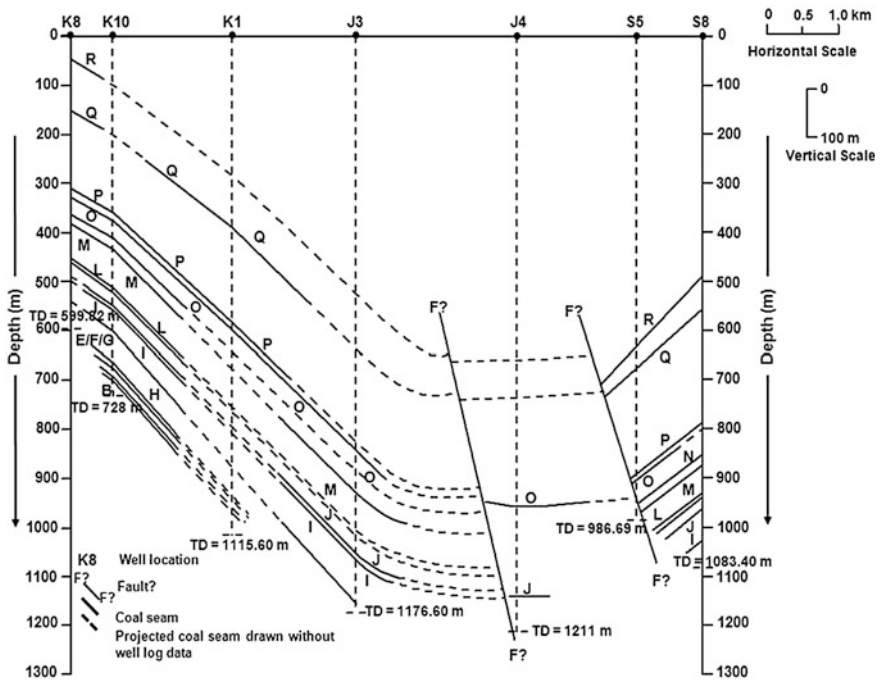


Fig. 4 Displaying schematic regional cross-section along section line K8-S8 (refer Fig. 3) in the Jharia coalfield, India (Chatterjee and Paul 2013). *TD* indicates total depth of well

Table 2 Seam-wise proximate analysis results for 10 wells of Jharia coalfield, India

| Seam name | Proximate analysis results (weight %) | | | |
|-----------|---------------------------------------|-------------|---------------------|------------------|
| | Moisture (%) | Ash (%) | Volatile matter (%) | Fixed carbon (%) |
| R | 1.05–1.21 | 17.86–26.38 | 19.50–24.84 | 50.41–55.09 |
| Q | 1.03–1.13 | 22.31–27.39 | 18.92–24.43 | 50.51–54.40 |
| P | 0.80–1.18 | 17.45–29.73 | 17.48–23.52 | 50.77–58.91 |
| O | 0.78–1.15 | 20.83–30.26 | 17.27–23.28 | 49.52–54.82 |
| N | 0.75–1.13 | 21.31–30.87 | 17.15–22.67 | 49.96–54.95 |
| M | 0.82–1.09 | 18.52–31.35 | 16.38–22.30 | 50.01–58.31 |
| L | 0.72–1.01 | 21.70–33.75 | 15.89–21.42 | 49.48–55.93 |
| K | 0.75–0.98 | 24.85–30.90 | 15.45–20.91 | 50.42–54.10 |
| J | 0.84–0.94 | 19.20–26.63 | 18.55–20.34 | 53.30–59.56 |
| I | 0.79–0.90 | 24.85–30.82 | 18.39–20.13 | 53.24–59.76 |
| H | 0.81–0.86 | 25.43–26.63 | 18.38–19.78 | 53.45–54.62 |
| E/F/G | 0.72–0.93 | 25.71–27.85 | 17.87–18.74 | 52.52–54.73 |
| D | 0.68–0.89 | 25.79–29.92 | 17.18–18.69 | 52.02–54.73 |
| C | 0.70–0.87 | 26.68–31.72 | 16.77–17.61 | 50.65–53.84 |
| B | 0.85 | 27.83 | 17.28 | 54.04 |

laboratory experiments. It can be inferred from proximate analysis that the moisture and volatile matter contents of coals gradually decreases with the increase of depth. The volatile matter content on dry ash free basis estimated by Rudra and Hazra (2009) indicates that the Barakar coals of Jharia coal basin are high volatile 'A' bituminous to low volatile bituminous in rank.

4 Petrographic Analysis of Coal in Laboratory

Coal petrographic analysis for 16 samples from 5 wells, namely, S15, K10, K16, K19, and K24 were carried out at the Central Institute for Mining and Fuel Research, Dhanbad following the Indian Standards (IS 9127 (Part 2) 2002; IS 9127 (Part 3) 2002; IS 9127 (Part 5) 2004). The seam-wise petrographic analysis results are presented in Table 3.

Figure 5 displays the cross-plot between vitrinite reflectance (VRO%) and depth of coal seams. On the basis of the available data, it is found that for the same coal seam VRO% values increases with increasing depth (as in seams I and M) and the VRO% values of coals in same well increases from younger to older coal seams (as in Wells S15, K10, K19 and K24).

Barakar coal seams are generally characterized by high vitrinite content although some coal seams are rich in inertinite content (Navale and Saxena 1989). For coal seam to hold and produce economic quantity of methane it should have vitrinite more than 45 % and VRO% should be more than 0.80 % along with low percentage of mineral matter and moisture (Kumar et al. 2010). From the present petrographic study and from the published data it is observed that vitrinite macerals are the major constituent of the coal of Jharia coal basin (Chatterjee et al. 1990; Mishra et al. 1990; Mishra and Cook 1992).

5 Estimation and Analysis of In-situ Stress

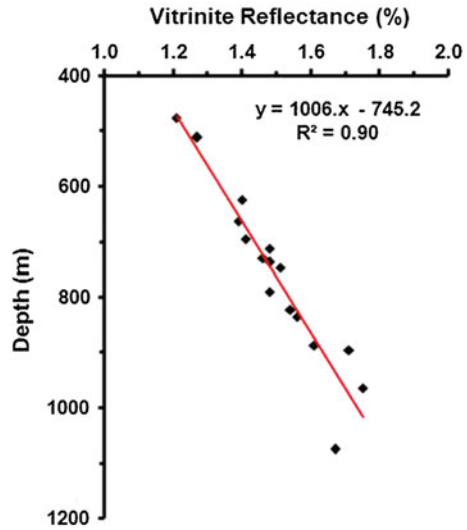
The magnitude of vertical stress/overburden load (S_v) at any depth is produced by the pressure exerted by the rocks above that particular point. The stresses (S_v) are computed by integrating density log values for wells where the hydrostatic pressure gradient with mud density 1.1 gm/cc is considered standard in the studied wells, drilled in both onshore and offshore areas. The pore pressure is assumed equal to the hydrostatic pressure at any particular depth during the estimation of effective stress. In this tectonically relaxed basin (Ghosh and Mukhopadhyay 1985), the effective minimum horizontal stress (S_h) has been estimated using the equation (Chatterjee and Pal 2010) provided below. From the present study it is possible to know the vertical stress magnitude at the roof of the individual coal seams.

Table 3 Laboratory derived coal petrography analysis results for 5 wells of Jharia coalfield, India

| Seam name | Well name | Coal core recovery depth interval (m) | Petrographic analysis results (volume % as received basis) | | | | | | | Mean VRo (%) |
|-----------|-----------|---------------------------------------|--|--------------------|---------------|----------------|--------------------|------|--|--------------|
| | | | Vitrinite (%) | Semi-vitrinite (%) | Liptinite (%) | Inertinite (%) | Mineral matter (%) | | | |
| R | S15 | 512.05–512.20 | 60.20 | 3.40 | 1.80 | 25.40 | 9.20 | 1.27 | | |
| Q | K19 | 477.45–477.55 | 65.50 | 2.90 | 1.80 | 25.10 | 4.70 | 1.21 | | |
| P | S15 | 834.57–834.76 | 50.50 | 2.30 | 1.10 | 37.60 | 8.50 | 1.56 | | |
| O | K16 | 729.65–729.55 | 52.30 | 2.70 | 0.00 | 39.70 | 5.30 | 1.46 | | |
| O | K19 | 696.04–696.14 | 63.40 | 2.60 | 0.90 | 29.60 | 3.50 | 1.41 | | |
| N | S15 | 964.25–964.35 | 44.40 | 1.23 | 1.00 | 40.60 | 12.77 | 1.75 | | |
| M | K10 | 624.80–624.95 | 61.60 | 2.40 | 1.20 | 29.80 | 5.00 | 1.40 | | |
| M | K24 | 663.25–663.65 | 58.80 | 6.40 | 1.90 | 24.40 | 8.50 | 1.41 | | |
| L | K24 | 737.75–737.85 | 60.70 | 1.90 | 0.30 | 30.70 | 6.40 | 1.48 | | |
| K | K10 | 712.65–712.75 | 58.90 | 2.10 | 0.80 | 33.80 | 4.40 | 1.48 | | |
| J | K24 | 790.30–790.40 | 46.30 | 5.60 | 0.40 | 39.50 | 8.20 | 1.49 | | |
| I | K10 | 747.45–747.55 | 57.50 | 1.90 | 0.60 | 35.80 | 4.20 | 1.51 | | |
| I | K16 | 886.75–886.85 | 46.30 | 2.10 | 0.30 | 48.20 | 3.10 | 1.61 | | |
| H | K24 | 822.95–823.10 | 42.10 | 5.10 | 0.20 | 45.40 | 7.20 | 1.54 | | |
| C | K16 | 1074.55–1074.70 | 44.60 | 1.10 | 0.20 | 51.80 | 2.30 | 1.67 | | |
| B | K10 | 895.85–896.00 | 16.10 | 1.10 | 0.00 | 69.70 | 13.10 | 1.71 | | |

VRo vitrinite reflectance

Fig. 5 Illustrates the plot of vitrinite reflectance versus depth



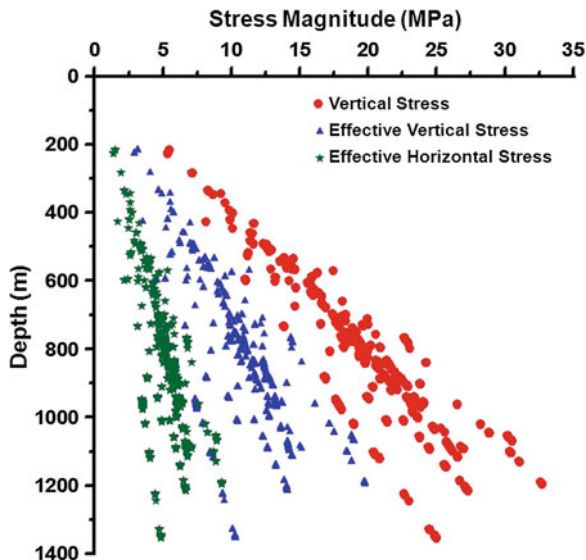
$$S_h = \gamma(S_v - P)/(1 - \gamma) \tag{1}$$

where ‘P’ is the pore pressure equivalent to hydrostatic pressure and ‘ γ ’ is the Poisson’s ratio of coal (0.32). It is known that Poisson Ratio for coal has variation with degree of cleating and it responds to stress field. From log data acquired in some wells penetrating Lower Gondwana coals in Jharia, Poisson’s ratio is computed generally varying in the range of 0.33–0.44 as a dynamic modulus for full observed range of degree of cleating. The value of 0.32 has been taken from laboratory studies. Owing to lack of fast shear and slow shear data, stress ratio determination is not possible.

Well logs of 30 wells from Jharia coalfield have been considered to determine the magnitudes of in-situ stresses of 16 major coal seams (considered seams E, F and G as a single E/F/G combined seam) of study area (Chatterjee and Paul 2013). Due to thin partings between seam E and F and seams F and G, these seams are considered as a single seam E/F/G during in-situ stress estimation. The magnitudes of S_v , effective vertical stress and effective horizontal stress are estimated and plotted against depth for the study area (Fig. 6).

A decrease in stress gradient is observed inside the coal seams (Fig. 7). The variation in stress gradient is dependent on density of rocks. It is also observed in few wells that the variations in stress gradients are also due the presence of high-density igneous intrusive rocks. The overall trend of the vertical stress increases linearly with depth with a slope of about 45°. This pattern is similar to that in the other coalfields of India and foreign coal basins (Mucho and Mark 1994; Townend and Zoback 2000). The estimated vertical stress, effective vertical stress and effective horizontal stress magnitudes are provided in Table 4 and vary between 5.31–32.71 MPa, 3.51–19.75 MPa and 1.35–9.29 MPa respectively within

Fig. 6 Showing magnitudes of vertical stress, effective vertical stress and effective horizontal stress against depth for 30 wells in Jharia coalfield



214.58–1345.04 m depth in the study area. The large variation of stress magnitude as observed, may be due to the high density igneous intrusive occurring close to the coal beds.

The variation in vertical stress magnitude values are also observed in each seam. The vertical stress magnitude contour maps are prepared for seams O, P, Q and R (Fig. 8). Four numbers of coal seams were selected for contour plotting, since

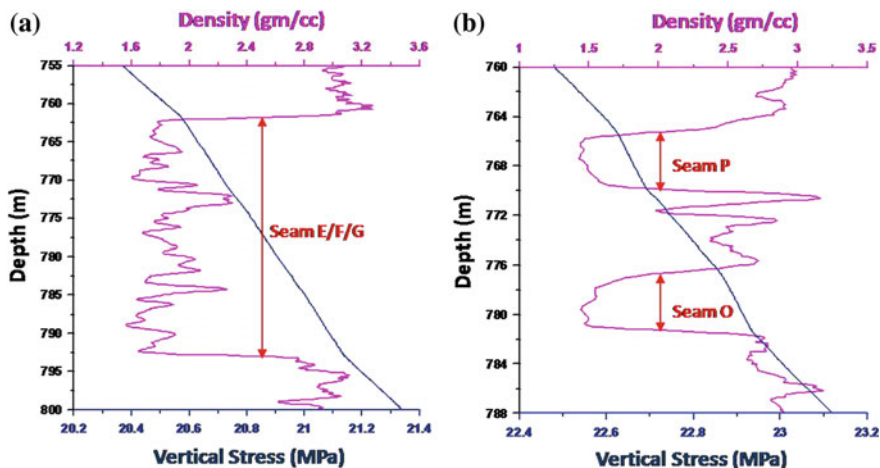


Fig. 7 Relationship between depth and vertical stress for **a** seam E/F/G in well K4 and **b** seam O and seam P in well K1

Table 4 The values of vertical stress, effective vertical stress, effective horizontal stress, coal bed permeability and gas content of study areas from Jharia coalfield, India

| Coalfield name | Seam name | Depth* (m) | | VS (MPa) | | EVS (MPa) | | EHS (MPa) | | CBP (md) | | GC (cc/gm) | |
|----------------|-----------|------------|---------|----------|-------|-----------|-------|-----------|------|----------|------|------------|-------|
| | | Min | Max | Min | Max | Min | Max | Min | Max | Min | Max | Min | Max |
| Jharia | A | 1214.52 | 1215.72 | 27.27 | 27.29 | 14.11 | 14.13 | 6.64 | 6.66 | NE | NE | NE | NE |
| Jharia | B | 842.28 | 1210.12 | 20.80 | 27.17 | 11.67 | 14.05 | 5.49 | 6.61 | NE | NE | 11.20 | 11.51 |
| Jharia | C | 831.18 | 1185.22 | 20.53 | 26.65 | 11.52 | 13.83 | 5.42 | 6.51 | 0.67 | 0.71 | 0.69 | 11.59 |
| Jharia | D | 802.28 | 1137.17 | 19.84 | 26.54 | 11.15 | 14.44 | 5.25 | 6.80 | 0.69 | 0.75 | 0.72 | 11.52 |
| Jharia | E/F/G | 762.08 | 1327.05 | 17.60 | 26.15 | 7.35 | 14.24 | 3.46 | 6.70 | 0.70 | 0.98 | 0.84 | 11.71 |
| Jharia | H | 720.58 | 788.07 | 17.98 | 24.84 | 10.07 | 13.62 | 4.74 | 6.41 | 0.76 | 0.80 | 0.78 | 11.69 |
| Jharia | I | 674.88 | 1244.05 | 16.85 | 32.71 | 9.47 | 19.75 | 4.46 | 9.29 | 0.60 | 0.85 | 0.73 | 11.89 |
| Jharia | J | 663.78 | 1345.04 | 16.60 | 31.05 | 9.33 | 18.80 | 4.39 | 8.85 | 0.64 | 0.97 | 0.81 | 11.91 |
| Jharia | K | 639.88 | 1102.86 | 15.98 | 30.43 | 9.04 | 18.46 | 4.26 | 8.69 | 0.69 | 0.88 | 0.79 | 11.72 |
| Jharia | L | 631.48 | 1098.46 | 15.80 | 30.38 | 8.96 | 18.44 | 4.22 | 8.68 | 0.74 | 0.92 | 0.83 | 11.61 |
| Jharia | M | 561.28 | 1100.95 | 14.00 | 28.85 | 7.92 | 17.52 | 3.73 | 8.24 | 0.76 | 1.05 | 0.91 | 11.72 |
| Jharia | N | 540.92 | 1019.46 | 13.54 | 28.23 | 7.66 | 17.16 | 3.61 | 8.08 | 0.77 | 0.98 | 0.88 | 11.86 |
| Jharia | O | 426.54 | 1117.04 | 8.14 | 30.52 | 3.51 | 18.93 | 1.65 | 8.91 | 0.65 | 1.25 | 0.95 | 11.75 |
| Jharia | P | 490.08 | 1052.67 | 12.30 | 30.26 | 6.61 | 18.80 | 3.11 | 8.85 | 0.72 | 1.08 | 0.90 | 11.67 |
| Jharia | Q | 282.78 | 837.47 | 7.10 | 24.22 | 4.04 | 15.13 | 1.90 | 7.12 | 0.81 | 1.13 | 0.97 | 11.68 |
| Jharia | R | 214.58 | 796.07 | 5.31 | 23.05 | 8.87 | 14.42 | 1.35 | 6.78 | 0.91 | 1.24 | 1.08 | 11.27 |

Depth* = depth of occurrence of coal seam; VS = vertical stress; EVS = effective vertical stress; EHS = effective horizontal stress; CBP = coal bed permeability; GC = gas content; Min minimum; Max maximum; Avg average and NE not estimated due to non-availability of well log data

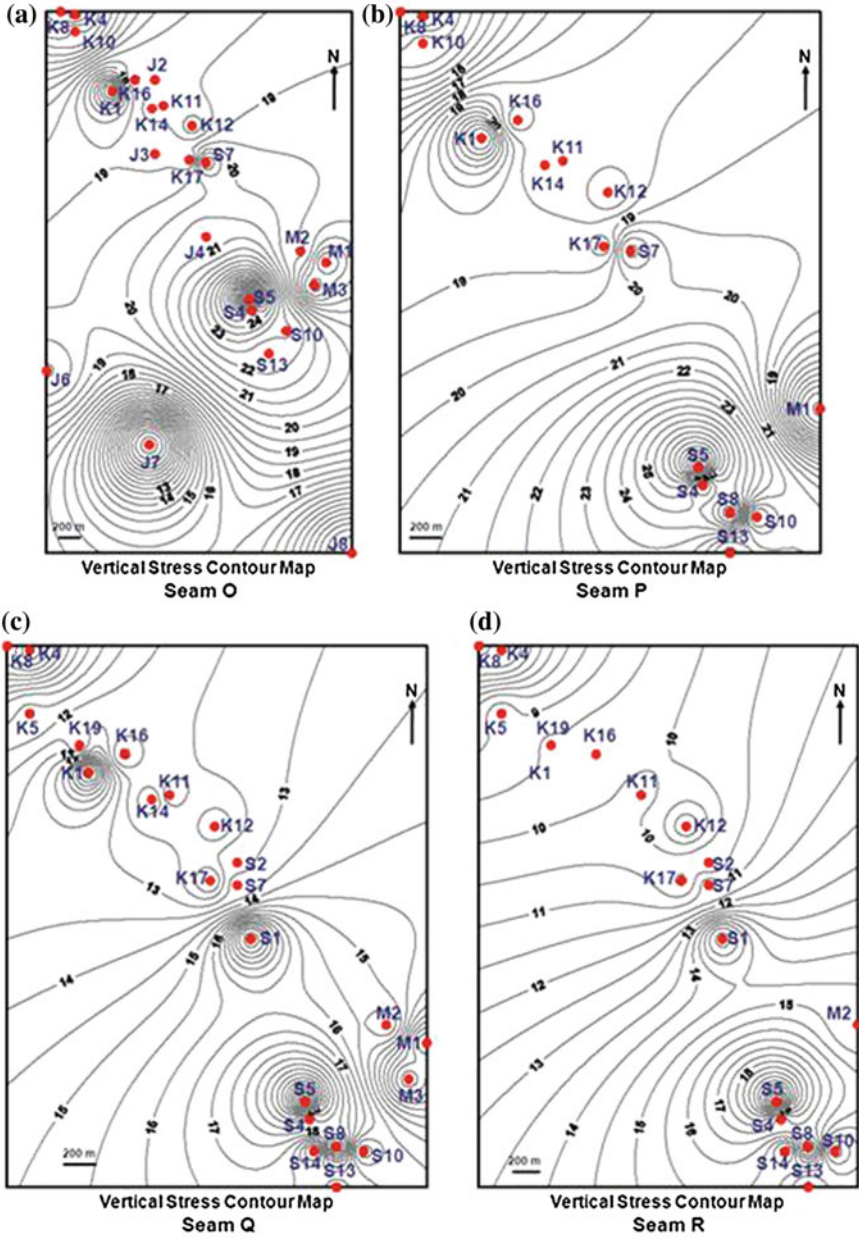


Fig. 8 Displaying vertical stress contour maps for **a** seam O, **b** seam P, **c** seam Q and **d** seam R. Vertical stress contour interval are considered as 0.5 MPa for all seams

majority of wells (sixteen to twenty three numbers of well) had penetrated these seams. The vertical stress magnitude for seam O increases from NNW to the centre part of the area and then decreases from the centre towards the SSE part of the area. This is due to the presence of greater sediment thickness as observed for the wells S4, S5, S10 and S13 located at the centre part of the basin. Vertical stress magnitude increases from NNW to SSE of the study area along the downdip direction and again increases from the central part of the basin along the updip direction. Stress magnitude for seams P, Q and R are increasing from NNW to SSE due to increase in sediment thickness and also due to the dipping coal beds in the same direction. Vertical stress magnitudes reach maximum at the central part of the study area where the wells like; S4, S5, S8, S10, S13 and S14 are located. Stress magnitude values decrease from the central part to the surrounding areas having lesser sediment thickness. The zones, marked by concentric high stress gradient, are generally separated by nala/river which are topographic manifestation of structural discontinuities like faults.

Cleats and fractures in coal of Barakar Formation in Jharia coalfield have already been mapped from coal outcrops from 21 opencast and 2 underground coal mines (Paul and Chatterjee 2011b). Face cleat orientation within same seams such as: B, C, D, E/F/G, H, I, J, K/L, N and O varies from NE–SW to NW–SE in different mining areas, distributed from NW to SE of the basin (Paul and Chatterjee 2011b). In-situ stress (S_H) orientation is parallel to the face cleat direction and has two prominent directions of N25°E and N25°W respectively. The S_H orientation is strongly related with the orientation of faults in this basin, between the major regional lineations, the face cleat and the joint direction (Paul and Chatterjee 2011b).

6 Estimation and Analysis of Coal Bed Permeability

Coal bed permeability (CBP) is almost due to cleat systems which are approximately orthogonal and are normal to the bedding plane. Cleat spacing ranges from millimeter to centimeter range. Coal permeability depends on the internal system of macroscopic (cleat) and microscopic (matrix), fractures, which are dependent on coal composition, coal rank, and timing of formation. Coal permeability depends not only on the volume of pores and fissures but also on the nature of their inter-connections. Any factor, that influences the geometry of pores and fissures, influences the permeability.

Coal seams are normally characterized by high electrical resistivities (500–4000 Ω -m). It had been observed that the resistivity measured by shallow resistivity logging tool across the coal seam decreases substantially in wellbores filled with high salinity fluids compared to wells with low salinity fluids (Yang et al. 2006). This indicated that the borehole fluid had replaced pore fluid in the cleats

(invasion zone). The cleat volume/porosity of cleated coal is given by the previous authors (Chatterjee and Pal 2010) as,

$$\text{Cleat volume or Porosity}(\Phi) = 100 \times (0.65/\text{Resistivity})^{0.6} \quad (2)$$

Using the matchstick model of cleating, initial porosity and initial permeability of coal in any coalfield area can be expressed as a function of cleat spacing and aperture (Harpalani and Chen 1995).

$$\text{Porosity}(\Phi) = 2b/s \quad \text{and} \quad \text{Permeability}(K) = b^3/12s \quad (3)$$

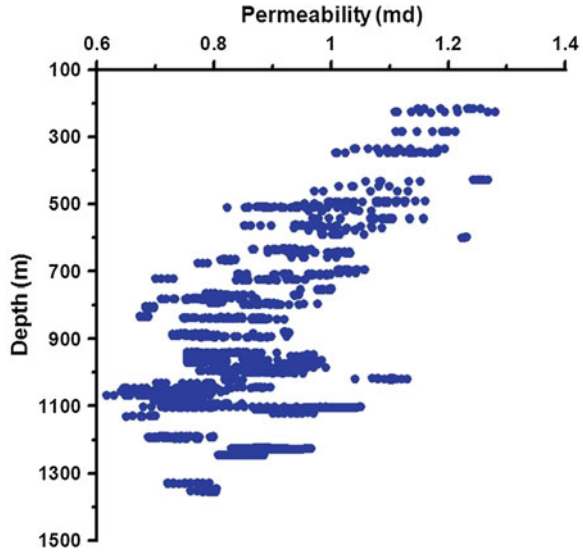
where 'b' and 's' are the cleat aperture and cleat spacing respectively.

This is the simplest possible model for estimating permeability. The formula used is the direct extension of permeability from flow between parallel plates extended to sets of them. Cleat spacing of 2 mm have been based on laboratory observation. Due to absence of correlating hydraulic aperture and cleat aperture (rugosity of cleat surface) we have assumed the equality between hydraulic aperture and cleat aperture (Gu and Chalaturnyk 2010). Cementation Exponent of 1.6 [1/1.6 = 0.6 in Eq. (2)] in porosity estimation from resistivity log is based on laboratory based correlations between resistivity index and saturating fluid resistivity from core samples in other wells in the area.

Short normal resistivity logs of the 16 wells namely; S1, S2, S4, S5, S7, S8, K1, K4, K5, K8, K12, J1, J3, J4, J7 and J8 have been considered for computation of permeability of 14 major coal seams, namely, seams C, D, E/F/G, H, I, J, K, L, M, N, O, P, Q and R. Resistivity log data for seams A and B are not available. During the field survey, the spacing between the mega face cleats were measured and found to be around 2–3 mm at the underground mines of West Jharia (WJ) and Putkee Bahihari (PB) areas (Paul and Chatterjee 2011a). Sahay (2009) had reported CBM gas emission from three wells, located in the extension area (Jarma block) of Moonidih. The coal bed permeability of the major seams, like K to R, in these three wells in the Moonidih area is reported less than 1 md (Sahay 2009). The interconnected cleated network has provided the coal bed permeability for fluid flow in the CBM reservoir for these wells under the study area. Therefore Eq. (3) has been used for computation of permeability from log derived cleat volume/porosity for the above mentioned 14 major coal seams of 16 wells with a cleat spacing of 2 mm. The estimated coal bed permeability is plotted against depth for the study area and it is observed that it decreases with increasing depth (Fig. 9).

The estimated coal bed permeability values of 16 wells in Jharia coalfield are predicted in Table 4. The average coal bed permeability of the study areas varies from 0.69 to 1.08 md in Jharia coalfield.

Fig. 9 Showing coal bed permeability against depth for 16 wells in Jharia coalfield



7 Relationship Between In-situ Stress and Coal Bed Permeability

The permeability of coal is affected by the strata stress, gas pressure and temperature of coal seam. The permeability change with respect to a reference state can be obtained from Eqs. (2) to (3) as proposed by several authors (e.g. Palmer and Mansoori 1998; Cui and Bustin 2005).

$$(K/K_0)^3 = (\Phi/\Phi_0)^3 \tag{4}$$

where the subscript 0 refers to the reference state and the matrix size change due to swelling/shrinkage and mechanical forces such as compression is considered as negligible compared to porosity change (Cui and Bustin 2005).

Cui and Bustin (2005) had defined the following stress-permeability relationship assuming constant pore compressibility and bulk compressibility \ll pore compressibility as

$$K = K_0 \exp(-3C_p \sigma_e) \tag{5}$$

where C_p = pore compressibility and σ_e = vertical effective stress.

It is a simplification to assume pore compressibility as stress-independent, but is reasonable in absence of laboratory data when regressions between effective vertical stress and permeability are confined seam wise and when large variation in vertical stress is absent. The above approach does not take into account variation in cleat space morphology in stressed state with respect to that in unstressed state. The

stress affecting on tortuosity is also not considered due to non-availability of relevant data. The type of resistivity measurement is likely to reflect mega cleats effects predominantly and also will be sensitive to both vertical and horizontal resistivity. In the given the data set of Jharia coalfield the approach is reasonable and the regression provides the relationship between coal bed permeability with effective vertical stress.

In Jharia coalfield, the relation between coal bed permeability and effective vertical stress magnitude for each of 4 wells namely; S7, S8, K4 and K12 has been illustrated in Fig. 10. These 4 wells have been chosen for plotting because these wells penetrated the major coal seams. The depth intervals for penetrated coal seams of wells S7, S8, K4 and K12 are 515.58–1092.68 m, 657.06–1195.96 m, 214.58–846.38 m and 345.76–970.26 m respectively. The goodness of fit (R^2) for best fit exponential curve between permeability and effective vertical stress for these 4 wells varies between 0.72 and 0.79.

Next, the coal bed permeability for four major seams (E/F/G, I, J, K) out of 14 seams are plotted with the effective vertical stress to display the variation pattern of permeability with effective vertical stress within the same seam. These seams were encountered in minimum of 3 wells. The change in permeability within the same coal seams with effective vertical stress are shown in Fig. 11a–d for seams E/F/G, I, J and K. Permeability of each coal seam decreases exponentially with the in-situ effective vertical stress. The R^2 values for the best fit exponential curve between permeability and effective vertical stress vary between 0.72 and 0.95.

Since no study on relationship between coal bed permeability and in-situ stress of coal seams of Jharia coalfield is found in public domain/available publications, till date, an attempt has been made to establish the same from this study. The permeability of all major coal seams for all 16 wells has been considered to decipher the relationship between coal bed permeability and effective vertical stress. A total of 3110 numbers of permeability and effective vertical stress data have been plotted to establish the best fit regression relationships. The exponential relationship between permeability and effective vertical stress has a correlation coefficient (r) of -0.80 and R^2 of 0.71 indicates reasonably good fit of the regression equation for this part of Jharia coalfield (Fig. 12). The cross-plot of permeability versus effective vertical stress in Fig. 12 represents the best fit regression equation for the central part of Jharia coalfield as:

$$y = 71.37e^{-2.22x}, \quad r = -0.80 \quad \text{and} \quad R^2 = 0.71 \quad (6)$$

where, y = permeability and x = well log derived effective vertical stress values.

Average coal bed permeability contour maps have been prepared for four seams namely; O, P, Q and R as displayed in Fig. 13. The four seams are chosen for permeability contour plotting because minimum of eight to maximum of eleven wells had penetrated these seams. The contour plots indicate the lateral variation of coal bed permeability of four seams. Average permeability data for coal seams O, P, Q and R indicate the anisotropic behavior of coal bed permeability. Figure 13a reveals predominant direction of the increase in permeability is along NNW-SSE.

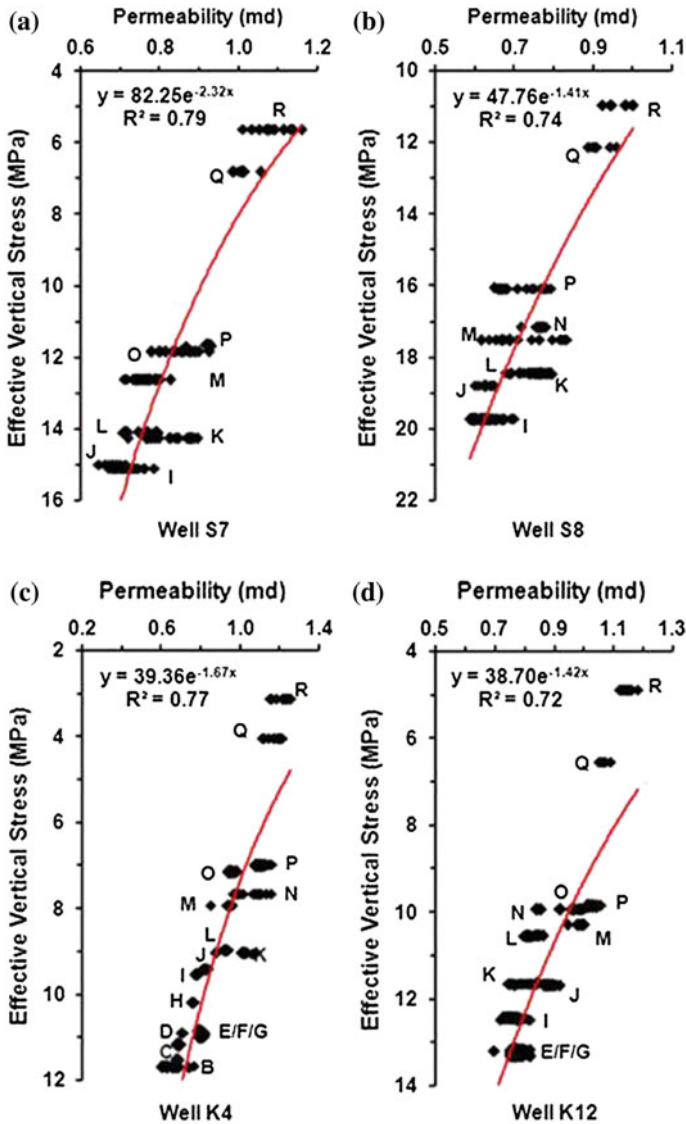


Fig. 10 Coal bed permeability versus effective vertical stress plots for **a** well S7, **b** well S8, **c** well K4 and **d** well K12. Name of the coal seams encountered are marked against respective wells

In case of seam O, a secondary direction of anisotropy was found along NE-SW direction (Fig. 13a). Average coal bed permeability for seam O increases towards updip direction from the central part of the area. The other Fig. 13b–d shows one dominant and another sub-dominant direction towards SSE-NNW and SSW-NNE direction respectively. The coal bed permeability depends on the cleat network

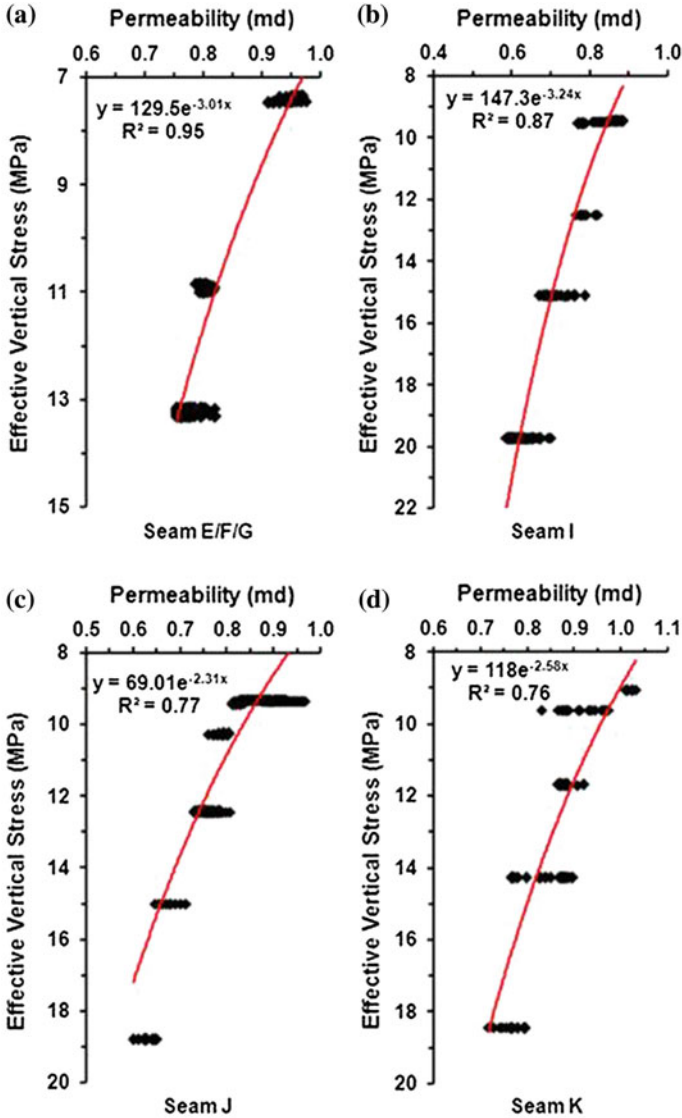
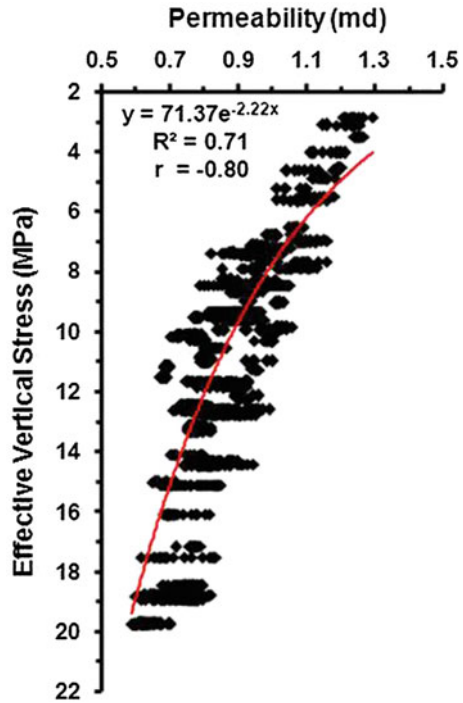


Fig. 11 Coal bed permeability versus effective vertical stress plots for **a** seam E/F/G, **b** seam I, **c** seam J and **d** seam K encountered in 16 wells distributed within Jharia coalfield

within these coal seams. In general fluid flow direction will follow the face cleat direction of the coal seams. Previously authors Paul and Chatterjee (2011a, b) had discussed the relation between cleat network and fluid flow directions at the Moonidih (WJ area mine) and Putkee-Balihari (PB area mine) underground mines and the adjoining areas of Jharia coalfield. The Moonidih and Putkee-Balihari underground mines are located very near to this study area (Fig. 3). The seam

Fig. 12 Coal bed permeability versus effective vertical stress plots considering all major coal seams encountered in 16 wells distributed within Jharia coalfield



permeability is higher along face cleat orientation of the major seams under study. The previous authors had also observed that the resultant face cleat and butt cleat orientations at these mines are aligned towards N15°W and N75°E respectively. The lineament study based on satellite imagery in Jharia coalfield and the directional analysis of lineaments in Moonidih area had indicated the most dominant trend towards NNW–SSE and secondary trend towards ENE-WSW (Tiwari and Rai 1996; Verma et al. 1989). Ali et al. (2008) had also observed that the face cleat orientation from formation micro- imagery (FMI) log in Parbatpur area is directed towards NW-SE direction, varying between N30°W and N60°W (Paul and Chatterjee 2011a). The present observation from the permeability contour plots for four seams conforms well with the previous studies. The coal bed permeability of the study area shows prominent increasing trend along SE-NW with maximum fluid flow direction from SE to NW.

8 Estimation of Gas Content from Well Logs

Sorption of gas by coal is considered as an extremely important area of research to enhance successful gas recovery from coal seams and to assist the understanding of gas-related problems in underground coal mining (Crosdale et al. 1998). Sorption of

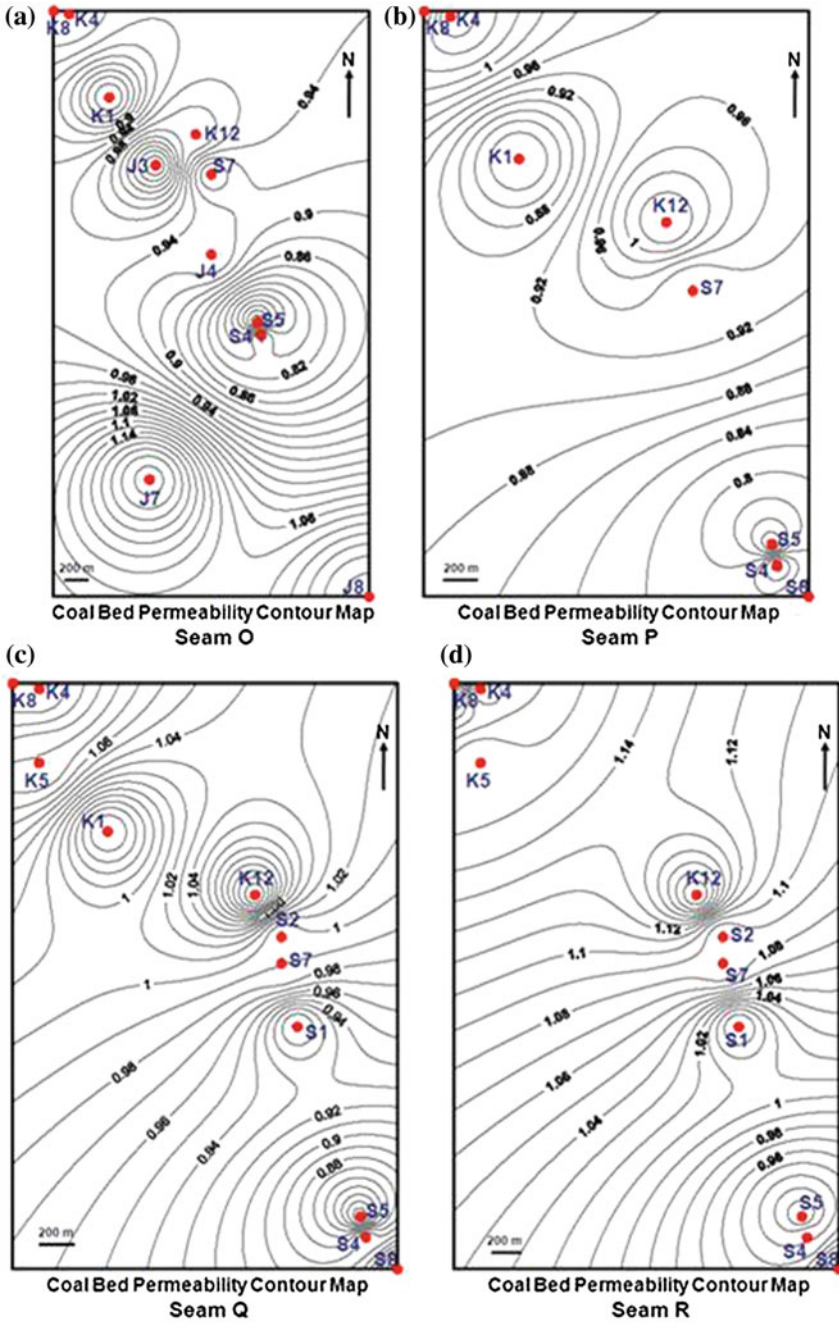


Fig. 13 Displaying coal bed permeability contour maps for **a** seam O, **b** seam P, **c** seam Q and **d** seam R. Coal bed permeability contour interval are considered as 0.02 md for seams O and P and 0.01 md for seams Q and R

gas by coal is robustly related with physical and chemical properties of coal (Crosdale et al. 1998). Gas in coal is adsorbed on the internal surface of micropores and varies directly with pressure and inversely with temperature. Previous authors like Bertard et al. (1970), Kissel et al. (1973), McKulloch et al. (1975), Diamond and Levine (1981), Feng et al. (1984) and Banerjee (1987) has proposed different direct methods for determination of methane adsorbed in coal beds. Gas content can also be estimated indirectly from any of the published global equations provided by Kim (1977), Mavor et al. (1993, 1995), Mullen (1988, 1991).

The above mentioned standard techniques/equations are mostly field-specific, so they alone may not be applicable for high confidence estimation of gas content of whole Jharia coalfield. Total gas in place (GIP) equals the product of tonnage of coal and gas content per unit weight of coal. By using density in g/cc units and gas content in cc/g units, the formula for the GIP calculation simplifies to the product of the volume of coal and a constant. The constant is different for each type of coal and is calculated as the product of the density in gm/cc and the gas content in cc/gm (for example, for a coal with density of 1.4 gm/cc and gas content of 4 cc/g, this constant is 5.6). Consequently, the formula we used is,

$$\text{GIP(Gas In Place)} = \text{Constant} \times \text{Volume}$$

where, Constant = Density (in g/cc) × Gas content (in cc/g).

The following equation is generally used to estimate the total initial adsorbed gas in a CBM reservoir:

$$G = 1359.7 Ah\rho_{ac}G_{ac}$$

where, G = Gas-in-Place in scf, A = Reservoir Area in acres, h = Thickness in feet, ρ_{ac} = Average In-situ Coal Density in gm/cc, G_{ac} = Average In-situ Gas Content in scf/ton.

Coal is a rock consisting largely of decomposed organic matter. Unlike most rock core, a coal core has a large internal surface area because it contains very small open pores within its structure. Most of the gas trapped within the coal adheres to the surfaces of the pores, and an estimation of the total internal surface area is useful for determining the potential for gas adsorption by the coal. Gas content per cc is a factor of microposity of coal, shape factor and is given by:

Gas content per cc = A * surface area per cc of coal = A * Available Microporosity of coal * shape factor of micropores * (1/micropore radius) = A * B * (Vitrinite Content/Factor of Degradation of microporosity due to blockage by mineral content) * shape factor of micropores * (1/micropore radius).

Degradation Factor is proportional to mineral content and can be considered as C * P_e * GR. This is so because mineral content will be of fine silt to clay size and radioactive and also will be containing elements having significant atomic number contrast with organics including volatiles.

Vitrinite content influences sonic slowness (Δt). It can be considered that

$$\text{Vitrinite content} = V * \Delta t$$

Adsorbed gas content per unit volume of coal can then be thought of as equaling $A * B * C * V * \Delta t / (P_e * GR) * (\alpha/r)$ where A, B, C, V are constants and α is shape factor of micro pores and r is micropore-radius, P_e = Photo-electric absorption index and GR = gamma ray response.

If ρ_c stands for coal density specific volume is given by $(1/\rho_c)$. Total gas content per unit mass of coal would be above plus non-adsorbed gas content say E, gas content per unit mass of coal is therefore given by

Gas content per unit mass of coal = $E + (A * B * C * V) * (\alpha/r) * (\Delta t / (P_e * GR * \rho_c))$ which has the form of the relation used in the paper as Eq. (4).

Parameter B changes with coal rank when same is higher than medium volatile bituminous. Dimension r also changes (decreases) with increasing coal rank. When coal rank is higher than medium volatile bituminous for the low values of radius of micropore and possible proximity of dimensions of mineral matter and micropores Factor C the damage factor increases with increasing rank. When coal rank is less than medium volatile bituminous then C tends to be fairly independent of mineral matter fraction and above formula holds good. Increasing mineral matter content is accompanied by decrease of gas capacity of coal for a given vitrinite content. Factor C increasing with increasing rank implies gas capacity of coal reducing with reducing mineral matter because as rank increases proximity of mineral matter size to micropore size increases, more than offsetting gain in available microporosity for lower mineral matter content.

Thus, the formula above is best suited for coal ranks equal to or lower than medium volatile bituminous rank. For higher ranks segmented parameterization of gas cc/gm of coal may give better estimates when such segmentation is carried out on the basis of vitrinite and ash content, and the form of parameterization would be expected to be different from Eq. (7).

Barakar coals of Jharia are high volatile bituminous to low volatile bituminous in rank. Coal seam wise regression will be useful with form above (since (α/r) can be different for different seams too) relation given in a concise form with the value of $(A * B * C * V) * (\alpha/r)$ and of E based on regression data carried, as per reference cited by Bhanja and Srivastava (2008) in the following Eq. (7).

Bhanja and Srivastava (2008) had proposed the methodology to predict gas content from well logs in Jharia coalfield in absence of the direct measurement of gas content data of coal samples. No gas adsorption data was available to know the gas content of the major seams encountered in the wells under study. Bhanja and Srivastava (2008) had established the relation between the well log parameters and gas adsorption data from the southern part of the Jharia coalfield. They had estimated the gas content for coal seams of Jharia coalfield from sonic, density, photo electric absorption index (P_e) and gamma ray logs from the following equation:

$$V = 0.767\{\Delta t/(\rho_c \times GR \times P_e)\} + 10.67 \quad (7)$$

where

V Volume of gas (cc/gm)

Δt Sonic log response for coal = 120 $\mu\text{s}/\text{ft}$ (for Jharia coalfield)

ρ_c Density log value for coal seam (gm/cc)

GR Gamma ray response for coal (cps)

P_e Photo-electric absorption index value for coal [1.8 barns/electron (for Jharia coalfield)]

For the present study, sonic log data were available for only 5 wells (J1, J3, J4, J7 and J8) adjacent to the Singra and Kapuria blocks and no photoelectric absorption index log (P_e) records were available for this study. Gas content has been estimated from the average sonic log response of 120 $\mu\text{s}/\text{ft}$ and an assumed P_e values from well log data for 30 wells (such as: S1, S2, S4, S5, S7, S8, S10, S13, S14, K1, K4, K5, K8, K10, K11, K12, K14, K16, K17, K19, M1, M2, M3, J1, J2, J3, J4, J6, J7 and J8) of Jharia coalfield. Table 4 lists the estimated range of average gas content values for 15 coal seams from these wells of Jharia coalfield. Gas content values range from 11.11 to 11.91 cc/gm for these seams.

9 Delineation of Most CBM Potential Zone

Comprehensive analysis and integrated study, as presented above, demonstrates that the present study area around central Jharia coalfield may be considered as a CBM potential zone in view of the reasonably high gas content values as estimated from well logs and merits consideration for further development. Since no directly measured gas adsorption data was available from within the study area, it is difficult to validate the log-derived gas contents with the actual gas content of these seams. To delineate major CBM potential zones gas content and coal seam thickness contour maps have been prepared for the seams O, P, Q and R only. In previous section coal bed permeability contour maps for the same four coal horizons have been explained. These four seams were selected for this study because these seams were penetrated by the maximum numbers of wells. Figures 14 and 15 represent the variation of gas content and coal seam thickness contour maps. By comparing gas content, coal seam thickness as well as coal bed permeability of these major coal seams, it is observed that the area containing the wells J3, J4, K12, S1, S2, S4, S5, S7 and S8 is having the coal bed permeability values ranging from 0.82 to 1.12 md with average gas content of 11.50–11.75 cc/gm. This zone is also situated in the deeper part of this study area as established in the previous section. Therefore, this zone may be considered as the most potential CBM zone (Fig. 3) and this zone may be targeted for further CBM exploration and production. It is to be noted that this zone is also adjacent to the Moonidih area containing wells M1, M2 and M3 and

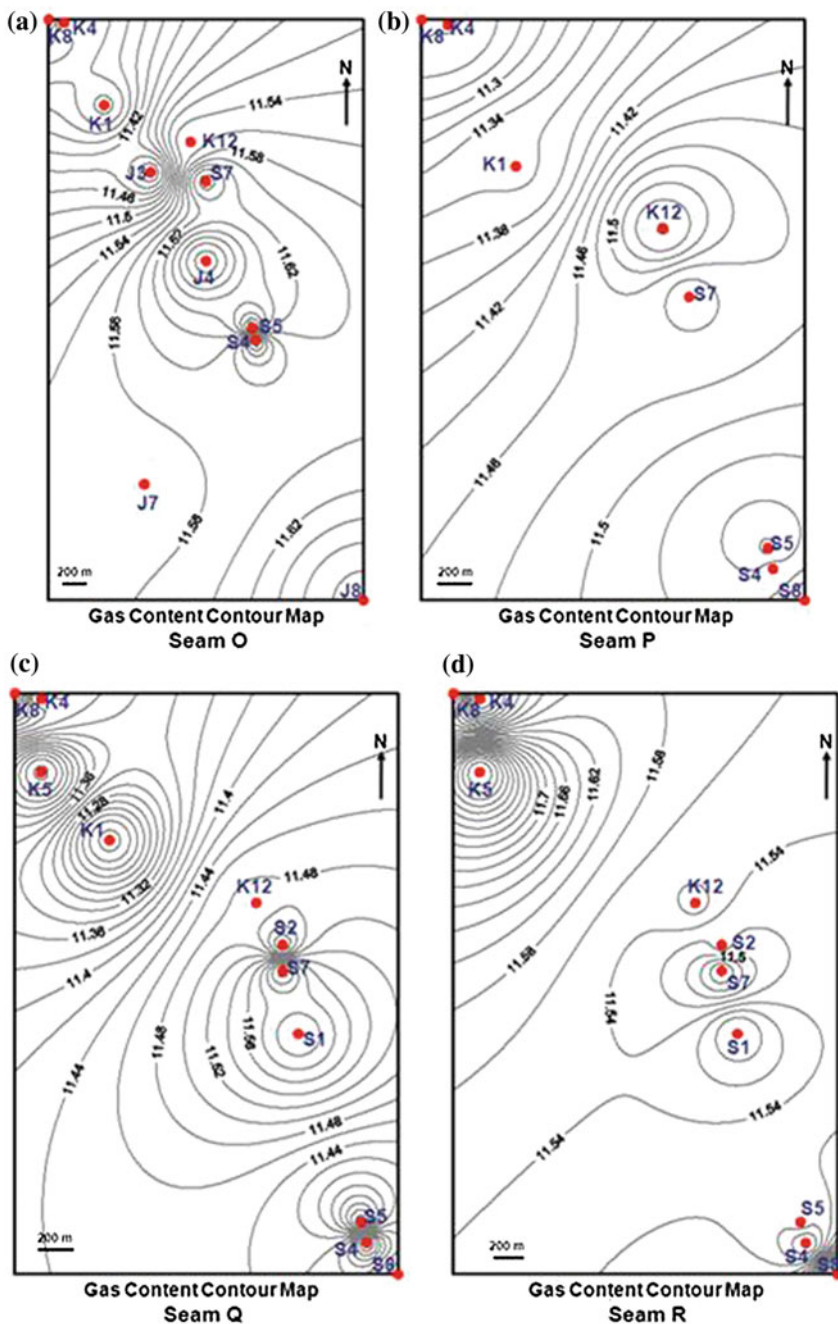


Fig. 14 Gas content contour maps for **a** seam O, **b** seam P, **c** seam Q and **d** seam R of Jharia coalfield, India. Gas content contour interval are considered as 0.02 cc/gm for all seams

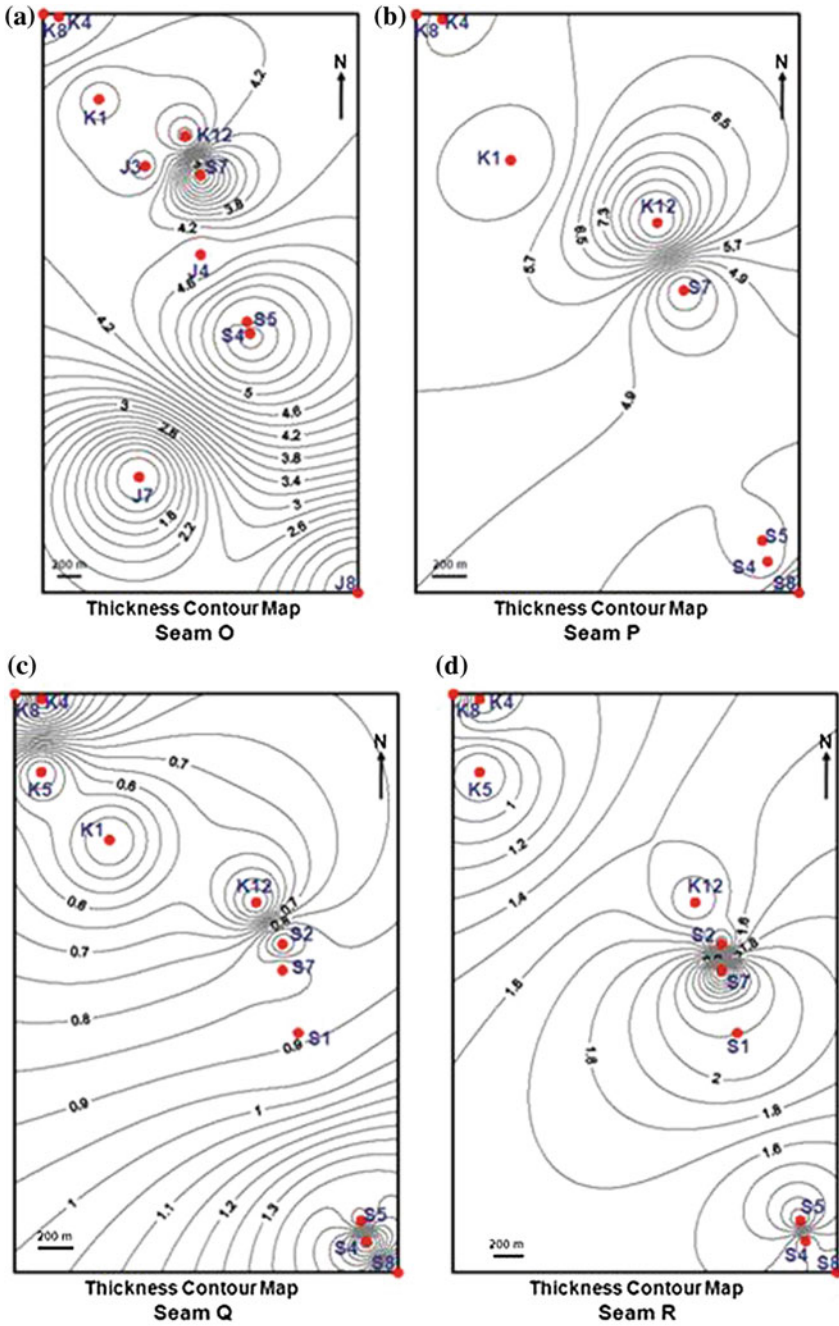


Fig. 15 Coal bed thickness contour maps for **a** seam O, **b** seam P, **c** seam Q and **d** seam R of Jharia coalfield, India. Coal bed thickness contour interval are considered as 0.20, 0.40, 0.10 and 0.10 m for seams O, P, Q and R respectively

Sahay (2009) had reported that the wells located in Moonidih area are producing CBM commercially. Therefore, it is inferred that the zone delineated from the present study may be taken up as the target for additional CBM investigation and potential production area.

10 Conclusions and Remarks

An integrated analysis has been carried out involving geological and geophysical well log data from 30 wells of the study area (Central Jharia coal basin), in combination with the data on proximate analysis, coal petrography, field mapping of cleat structures and lineaments of the area. The study aimed to estimate the critical reservoir parameters of coal seams as CBM reservoir and also to identify the most potential zone for CBM development. The findings for the study area are summarised below:

The stress magnitudes have been computed from the well log data and relationships between depth and vertical stress, effective vertical stress and effective horizontal stress have been established. All the values show increasing trend with depth with varying gradient (Fig. 6; Table 4).

It is observed that the gradient of effective vertical stress reduces within the coal seams due to change in density compared to the roof and floor rocks (Fig. 7). Vertical stress contour maps at the seam roofs show that the stress increases towards the dip of the inclined strata, i.e., towards the deeper or central part of the basin (Fig. 8). The vertical stress contour maps also reveal that the primary direction of stress anisotropy is along NW-SE direction (Fig. 8). It is also observed that the occurrence of high gradient anomalous zones are associated with the major geological structural discontinuities and local lineament pattern.

Coal bed permeability was calculated for each major coal seam from matchstick model using available standard equations. The coal bed permeability values range between 0.69 and 1.08 md. The plots of permeability values against depth show a linear decreasing trend with increasing depth (Fig. 9). The relationship between effective vertical stress (EVS) and permeability is also established and an empirical equation (Eq. 6) has been derived where the correlation co-efficient is 0.71. It is also established that the coal seam permeability progressively decreases with increasing EVS (Figs. 10, 11 and 12).

In order to delineate the CBM potential zones and direction of higher permeability, contour maps for four major coal seams have been generated. The direction of higher permeability lies to the NW and predicted direction of gas flow in from SE to NW. A secondary direction along ENE to WSW has also been found (Fig. 13) and these results are showing close consistency with some previous regional studies.

Gas content values were computed from sonic, density, gamma ray log and photo-electric absorption index logs (Eq. 7; Table 4). Gas content estimated are found to vary between 11.11 and 11.91 cc/gm. Considering the critical parameters

for CBM reservoir such as permeability, stress orientation and gas content, the area encompassing wells—J3, J4, K12, S1, S2, S4, S5, S7 and S8 is found to be most potential (Fig. 3). It may be considered as target for further CBM exploration and production project around this area.

A richer well log data suite including electrical high resolution images: radial and azimuthal delineated shear slowness, Stoneley waveform inversion, energy attenuation and nuclear magnetic resonance (NMR) supported by elemental dry weight logs help filling the vital knowledge gaps for characterization at wells and focused mapping. These further would guide not only locations for sinking wells but also type of wells, well trajectory design, stimulation where required and completion strategies needed for maximizing economic benefits and sustained gain.

Acknowledgments The authors express their sincere gratitude to Coal India Limited (CIL), India and Central Mine Planning and Design Institute Limited (CMPDIL), Ranchi, India for the financial assistance under its R&D scheme.

References

- Ali M, Sarkar A, Sagar R, Klimentos T, Basu I (2008) Cleat characterization in CBM wells for completion optimization. In: SPE indian oil and gas technical conference and exhibition, Mumbai, India, 4–6 March 2008 (Paper Id. SPE 113600)
- Banerjee BD (1987) A new approach to the determination of methane content of coal seams. *Int J Min Geol Eng* 5:369–376
- Bell JS, Bachu S (2003) In-situ stress magnitude and orientation estimates for Cretaceous coal-bearing strata beneath the plains area of central and southern Alberta. *Bull Can Pet Geol* 51(1):1–28
- Bertard C, Bruyet B, Gunther J (1970) Determination of desorbable gas concentration of coal (direct method). *Int J Rock Mech Min Sci* 7:43–65
- Bhanja AK, Srivastava OP (2008) A new approach to estimate CBM Gas Content from well logs. In: SPE Asia Pacific oil and gas conference and exhibition, Perth, Australia, 20–22 Oct 2008 (Paper Id. SPE 115563)
- Chandra D (1992) Jharia coalfield. *Mineral Resources of India*, Geological Society of India, Bangalore, pp 1–149
- Charles MBII, Bai Q (1998) Methodology of coalbed methane resource assessment. *Int J Coal Geol* 35(1–4):349–368
- Chatterjee R, Pal PK (2010) Estimation of stress magnitude and physical properties for coal seams of Rangamati area, Raniganj coalfield, India. *Int J Coal Geol* 81:25–36
- Chatterjee R, Paul S (2013) Classification of coal seams for coal bed methane exploitation in central part of Jharia coalfield, India—a statistical approach. *Fuel* 111:20–29
- Chatterjee CN, Ghose S, Chandra D (1990) Micropetrographic characteristics of certain Lower Permian coal seams of India with special reference to their mode of formation. *Int J Coal Geol* 14:295–308
- Close JC (1993) Natural fractures in coal. In: Law BE, Rice DD (eds) *Hydrocarbons from coal*. AAPG studies in geology, vol 38, pp 119–132
- Crosdale PJ, Beamish BB, Vlix M (1998) Coalbed methane sorption related to coal composition. *Int J Coal Geol* 35:147–158
- Cui X, Bustin RM (2005) Volumetric strain associated with methane desorption and its impact on coalbed gas production from deep coal seams. *AAPG Bull* 89(9):1181–1202

- Diamond WP, Levine JR (1981) Direct method determination of the gas content of coal: procedures and results. US Bureau of Mines report of investigations, RI 8515
- Feng KK, Cheng KC, Augsten R (1984) Preliminary evaluation of the methane production potential of coal seams at Greenhills Mine, Elkford, British Columbia. *CIM Bull* 77:56–60
- Ghosh SK, Mukhopadhyay A (1985) Tectonic history of the Jharia Basin—an intracratonic Gondwana basin of Eastern India. *Q J Geol Min Metall Soc India* 57:33–58
- Gu F, Chalaturnyk RJ (2010) Permeability and porosity models considering anisotropy and discontinuity of coalbeds and application in coupled simulation. *J Petrol Sci Eng* 74(3–4):113–131
- Harpalani S, Chen G (1995) Estimation of changes in fracture porosity of coal with gas emission. *Fuel* 74(10):1491–1498
- Harpalani S, Schraufnagel RA (1990) Shrinkage of coal matrix with release of gas and its impact on permeability of coal. *Fuel* 69:551–556
- Hazra PN, Rudra M, Guha S, Kar MK, Basumatary JK, Kumar A. (2003) Geochemical characterization of Coalbed Gas of Jharia & Raniganj Basins and its implications. In: Proceedings of international conference, Mussauri, India
- IS 1350 (Part 1) (2003) Indian standard methods of test for coal and coke. Part 1: proximate analysis. Bureau of Indian Standards, 2nd revision, pp 1–28
- IS 436 (Part 1/Section 1) (1991) Indian standard methods for sampling of coal and coke, Part 1: sampling of coal, Section 1: manual sampling. Bureau of Indian Standards, 8th reprint, pp 1–28
- IS 9127 (Part 2) (2002) Indian standard methods for the petrographic analysis of bituminous coal and anthracite. Part 2: method of preparing coal samples. Bureau of Indian Standards, 1st revision, pp 1–8
- IS 9127 (Part 3) (2002) Indian standard methods for the petrographic analysis of bituminous coal and anthracite. Part 3: method of determining maceral group composition. Bureau of Indian Standards, 1st revision, pp 1–6
- IS 9127 (Part 5) (2004) Indian standard methods for the petrographic analysis of bituminous coal and anthracite. Part 5: method of determining microscopically the reflectance of Vitritinite. Bureau of Indian Standards, 1st revision, pp 1–12
- Kim AG (1977) Estimating methane content of bituminous coal beds from adsorption data. U.S. Bureau of Mines, RI 8245, pp 1–22
- Kissell FN, McCulloch CM, Elder CH (1973) The direct method of determining methane content of coal beds for ventilation design. US Bureau of Mines Report of Investigations, RI 7767
- Kumar A, Singh SK, Datta GC (2010) Petrographic characteristics of Gondwana coals of Barakar formation of Bokaro CBM block, Jharkhand, India—implications on certain critical parameters. In: Proceedings of 9th international oil & gas conference and exhibition (PETROTECH 2010), New Delhi, India, 31 October–3 Nov 2010 (Paper Id 20100094)
- Laubach SE, Marrett RA, Olson JE, Scott AR (1998) Characteristics and origins of coal cleat: a review. *Int J Coal Geol* 35:175–207
- Law BE (1993) The relation between coal rank and cleat spacing: implications for the prediction of permeability in coal. Proceedings of international coalbed methane symposium II:435–442
- Li H, Ogawa Y, Shimada S (2003) Mechanism of methane flow through sheared coals and its role on methane recovery. *Fuel* 82:1271–1279
- Mavor MJ, Close JC, McBane RA (1993). Formation evaluation of exploration coalbed methane wells. SPE/CIM joint international meeting, Calgary, 10–13 June (Paper Id. SPE 21589)
- Mavor MJ, Pratt TJ, Nelson CR (1995) Quantify the accuracy of coal seam gas content. *Petrol Eng Int* 68(10):37–42
- McCulloch CM, Levine JR, Kissell FN, Deul M (1975) Measuring the methane content of bituminous coal beds. US Bureau of Mines report of investigations RI 8043
- Mishra HK, Cook AC (1992) Petrology and thermal maturity of coals in the Jharia Basin: implications for oil and gas origins. *Int J Coal Geol* 20(3–4):277–313
- Misra BK, Singh BD, Navale GKB (1990) Resino-inertinites of Indian Permian coals—their origin, genesis and classification. *Int J Coal Geol* 14:277–293

- Mucho TP, Mark C (1994) Determining horizontal stress direction using stress mapping technique. In: Proceedings of 13th international conference on ground control in mining, Morgantown, pp 277–289
- Mullen MJ (1988) Log evaluation in wells drilled for coal-bed methane. Rocky Mountain Association of Geologists, pp 113–124
- Mullen MJ (1991) Coalbed methane resource evaluation from wireline logs in northeastern San Juan Basin: a case study. SPE joint rocky mountain regional/low permeability reservoirs symposium and exhibition, Denver, Colorado, 6–8 March, pp 161–172 (Paper Id. 18946)
- Navale GKB, Saxena R (1989) An appraisal of coal petrographic facies in Lower Gondwana (Permian) coal seams of India. *Int J Coal Geol* 12:553–588
- Palmer I, Mansoori J (1998) How permeability depends on stress and pore pressure in coalbeds, a new model. *SPE Reservoir Eval Eng* 1(6):539–544
- Pashin JC (1998) Stratigraphy and structure of coalbed methane reservoirs in the United States: an overview. *Int J Coal Geol* 35:209–240
- Pashin JC, Groshong RH Jr (1998) Structural control of coalbed methane production in Alabama. *Int J Coal Geol* 38:89–113
- Paul S, Chatterjee R (2011a) Determination of in-situ stress direction from cleat orientation mapping for coal bed methane exploration in south-eastern part of Jharia coalfield, India. *Int J Coal Geol* 87:87–96
- Paul S, Chatterjee R (2011b) Mapping of cleats and fractures as an indicator of in-situ stress orientation, Jharia coalfield, India. *Int J Coal Geol* 88:113–122
- Pitman JK, Pashin JC, Hatch JR, Goldhaber MB (2003) Origin of minerals in joint and cleat systems of the Pottsville Formation, Black Warrior basin, Alabama: implications for coalbed methane generation and production. *AAPG Bull* 87(5):713–731
- Rudra M, Hazra PN (2009) Isotopic composition of coalbed methane desorbed from Barakar coals of Damodar valley Gondwana coalfields and its implication. In: Proceedings of petrotech, 11–15 Jan, New Delhi, India
- Sahay AN (2009) CMM demonstration project at Moonidih: a path finder for CMM development in Indian geo-mining scenario. *MineTech* 30(4):11–17
- Sengupta N (1980) A revision of the geology of the Jharia coalfield with particular reference to distribution of coal seams. Ph.D. thesis, Indian School of Mines, Dhanbad
- Tiwari A, Rai B (1996) Hydromorphogeological mapping for groundwater prospecting using landsat-MSS images—a case study of part of Dhanbad District, Bihar. *Journal of the Indian Society of Remote Sensing* 24(4):281–285
- Townend J, Zoback MD (2000) How faulting keeps the crust strong. *Geology* 28:399–402
- Verma RP, Jaipurian AM, Paul PR (1989) Compendium on updated and revised geology of Jharia coalfield (excluding TISCO). Central Mine Planning and Designing Institute Ltd., Ranchi, pp 1–282
- Yang Y, Peters M, Cloud TA, Van Kirk CW (2006) Gas productivity related to cleat volumes derived from focused resistivity tools in coalbed methane (CBM) fields. *Petrophysics* 47(3):250–257